

# A computational investigation of H<sub>2</sub> adsorption and dissociation on Au nanoparticles supported on TiO<sub>2</sub> surface

Andrey Lyalin,<sup>1</sup> and Tetsuya Taketsugu

*Division of Chemistry, Graduate School of Science,  
Hokkaido University, Sapporo 060-0810, Japan.  
E-mail: lyalin@mail.sci.hokudai.ac.jp*

The specific role played by small gold nanoparticles supported on the rutile TiO<sub>2</sub>(110) surface in the processes of adsorption and dissociation of H<sub>2</sub> is discussed. It is demonstrated that the molecular and dissociative adsorption of H<sub>2</sub> on Au<sub>n</sub> clusters containing n = 1, 2, 8 and 20 atoms depends on cluster size, geometry structure, cluster flexibility and the interaction with the support material. Rutile TiO<sub>2</sub>(110) support energetically promotes H<sub>2</sub> dissociation on gold clusters. It is demonstrated that the active sites towards H<sub>2</sub> dissociation are located at corners and edges on the surface of the gold nanoparticle in the vicinity of the support. The low coordinated oxygen atoms on the TiO<sub>2</sub>(110) surface play a crucial role for H<sub>2</sub> dissociation. Therefore the catalytic activity of a gold nanoparticle supported on the rutile TiO<sub>2</sub>(110) surface is proportional to the length of the perimeter interface between the nanoparticle and the support.

## 1 Introduction

Since the pioneering work of Haruta on the oxidation of carbon monoxide by small gold nanoparticles supported by metal oxides,<sup>1</sup> an extensive interest has been devoted to understanding the catalytic properties of gold. Such an interest is stipulated by the fact that gold nanoparticles are active even at room temperatures that makes them unique catalysts for many industrial applications.<sup>2,3</sup>

---

<sup>1</sup>On leave from: V. A. Fock Institute of Physics, St Petersburg State University, 198504 St Petersburg, Petrodvorez, Russia.

The most explored type of catalytic reactions with gold nanoparticles are reactions of oxidation and epoxidation, including the oxidation of carbon monoxide at mild temperatures, alcohol oxidation, the direct synthesis of hydrogen peroxide and alkene epoxidation; see, e.g., refs. 1,4–10 and references therein. In spite of intensive theoretical and experimental studies the origin of catalytic activity of gold remains highly debated.

It is commonly accepted that several factors can influence the catalytic activity of gold. The most important factor is the size effect. It has been shown that the unique properties of gold in oxidation reactions emerge when the size of catalytic particles decreases down to 1-5 nm or even less; while larger sized particles and the bulk form of gold are catalytically inactive.<sup>1,4,5,7</sup> It has been shown that small gold clusters consisting of a few atoms can also possess extraordinarily high catalytic activity.<sup>11,12</sup> On the one hand, the size effects in gold nanocatalysis are determined by quantum effects, resulting from the spatial confinement of the valence electrons in the cluster;<sup>13</sup> on the other hand, in such clusters a dominant fraction of atoms are under-coordinated (in comparison with the bulk), hence they exhibit an enhanced chemical reactivity.<sup>13–15</sup>

Interaction with the support material is another important factor that considerably influences the chemical reactivity of the gold nanoparticles.<sup>4,16–18</sup> Most experimental studies on the catalytic properties of gold have been performed for gold nanoparticles supported on the surfaces of metal oxides; see, e.g., refs. 4,19 and references therein. It has been demonstrated that the catalytic activity of gold nanoparticles depends on the presence of defects in the support material (e.g. F-center defects), charge transfers from the support, the chemical state of the surface, doping, moisture, special additives, and the presence of adsorbates on the cluster surface, including the reactant molecule itself; see, e.g., refs. 4,10,16,19–24 and references therein. However, a work by Turner *et al.* presents strong experimental evidence that small gold entities ( $\sim 1.4$  nm) derived from Au<sub>55</sub> clusters and deposited on an inert support can also be efficient and robust catalysts for oxidation reactions.<sup>5</sup> Hence, the interaction with the support is important but not the determining factor in catalytic activity of gold; therefore even free clusters can be effective catalysts.

Heterogeneously catalyzed hydrogenation is another type of reactions where gold nanoparticles have shown their great potential as catalysts. It has been demonstrated experimentally that gold nanoparticles supported on metal oxides such as SiO<sub>2</sub>, Al<sub>2</sub>O<sub>3</sub>, TiO<sub>2</sub>, ZnO, ZrO<sub>2</sub>, and Fe<sub>2</sub>O<sub>3</sub> are effective catalysts for selective hydrogenation of several classes of organic molecules, including  $\alpha$ ,  $\beta$ -unsaturated aldehydes, unsaturated ketones, and unsaturated hydrocarbons.<sup>25–34</sup>

Moreover, supported gold nanoparticles are very selective for the direct formation of hydrogen peroxide from  $\text{H}_2/\text{O}_2$  mixtures.<sup>8</sup> Mechanisms of such catalytic reactions are largely not understood. Experimental results demonstrate that molecular hydrogen does not bind to the clean gold extended surface, and molecular or dissociative hydrogen adsorption occurs on the supported gold nanoparticles.<sup>32,35</sup> It has been suggested that hydrogen reacts and dissociates on low coordinated gold atoms in the corner or at edge positions on the surface of gold nanoparticles.<sup>30,35</sup> It has been also shown that the shape of the gold particles plays a role on their catalytic activity.<sup>36</sup> However, in a recent work by Haruta *et al* it has been found that the catalytic activity of the gold nanoparticles supported on the rutile  $\text{TiO}_2(110)$  surface depends on the number of gold atoms located at the perimeter interface of the supported gold nanoparticles, irrespective of the cluster size.<sup>37</sup> It was also supposed that active sites for  $\text{H}_2$  dissociation may be formed by a combination of gold atoms and oxygen atoms from  $\text{TiO}_2$  at nanoparticle–surface interface.<sup>37</sup>

Surprisingly, very little attention has been paid to theoretical investigations of the hydrogenation reactions on gold nanoparticles. Interaction of molecular hydrogen with gold atoms and small gold clusters has been theoretically studied in refs. 38–45. It has been demonstrated, that the flexibility of the cluster structure plays a key role in the bonding and dissociation of  $\text{H}_2$  on  $\text{Au}_{14}$  and  $\text{Au}_{29}$ .<sup>43</sup> Furthermore, authors in ref. 43 have concluded that dissociation of  $\text{H}_2$  is only possible when a cooperation between four active low coordinated Au atoms on the cluster surface is allowed. However, in ref. 46 the compelling evidence has been presented that  $\text{H}_2$  adsorbs and dissociates with small activation barriers on low coordinated Au atoms situated in corner positions of different  $\text{Au}_{25}$  nanoparticles without further conditions. Thus, there is no need for cooperation between several active Au atoms to dissociate  $\text{H}_2$  and dissociation can occur spontaneously on a single low coordinated Au atom, when coordination number is four.<sup>46</sup>

There are relatively few theoretical studies on the catalytic hydrogenation reactions on gold clusters. These include works on formation of hydrogen peroxide from  $\text{H}_2$  and  $\text{O}_2$  over small gold clusters;<sup>47,48</sup> acrolein hydrogenation on  $\text{Au}_{20}$  nanoparticle;<sup>49</sup> and combined experimental and theoretical investigation of the unusual catalytic properties of gold nanoparticles in the selective hydrogenation of 1,3-butadiene toward cis-2-butene.<sup>50</sup>

Despite of the clear experimental evidence indicating a strong influence of the support materials on the processes of adsorption and dissociation of molecular hydrogen and related hydrogenation processes on the supported gold nanoparticles,<sup>32,37</sup> there are no theoretical studies concerning the role of the support with an exception of recent works by Boronat *et al*.<sup>51</sup> and Florez *et al*.<sup>52</sup> In ref. 51

authors performed an elegant theoretical study on elucidation of active sites for  $\text{H}_2$  adsorption and activation on  $\text{Au}_{13}$  cluster supported on the anatase  $\text{TiO}_2$  (001) surface. It has been shown that Au atoms that are active for  $\text{H}_2$  dissociation must have a net charge close to zero, be located at corner or edge low coordinated positions, and not be directly bonded to the support.<sup>51</sup> The  $\text{Au}_{13}$  isomers consisting of two layers of gold atoms have the largest number of potentially active sites where  $\text{H}_2$  can be adsorbed and activated. These active atoms are located on the top layer of the  $\text{Au}_{13}$  cluster that does not have contact with the support.<sup>51</sup> It has been demonstrated that the presence of O vacancy defects on the anatase  $\text{TiO}_2$  (001) surface can stabilize the most active two-layer  $\text{Au}_{13}$  particles.<sup>51</sup> In ref. 52 it was shown that small two-dimensional Au nanoparticles supported on TiC(001) can dissociate  $\text{H}_2$  in a more efficient way than when supported on oxides. The active sites for  $\text{H}_2$  dissociation on Au/TiC(001) are located at the particle edge and in direct contact with the underlying substrate.<sup>52</sup>

In the present paper we report the results of a systematic theoretical study of the adsorption and dissociation of  $\text{H}_2$  on free and  $\text{TiO}_2$ (110) supported  $\text{Au}_n$  clusters containing  $n = 1, 2, 8$  and 20 atoms. In our work we want to clarify how hydrogen molecule adsorbs and dissociates on the gold nanoparticles. What factors are the most important for  $\text{H}_2$  dissociation on the surface of gold? Does the dimensionality of the cluster play a role in  $\text{H}_2$  adsorption and dissociation? What is the role of the support? Is it possible to promote dissociation of  $\text{H}_2$ ? Whether or not the charge transfer between the adsorbed  $\text{H}_2$  and the gold cluster plays any role in  $\text{H}_2$  catalytic activation and dissociation? Why the catalytic activity of gold nanoparticles supported on the rutile  $\text{TiO}_2$ (110) surface depends on the number of gold atoms located at the perimeter interface, irrespective to the particle size in the case of  $\text{H}_2$  dissociation, but it depends on cluster size in the case of  $\text{O}_2$  dissociation? Finally, what are the important directions for further theoretical investigation of the considered processes? Answering these questions is the central aim of the present work.

## 2 Computational Details

The calculations are carried out using density-functional theory (DFT) with the gradient-corrected exchange-correlation functional of Perdew, Burke and Ernzerhof (PBE).<sup>53</sup> The atom-centered, strictly confined, numerical basis functions<sup>54,55</sup> are used to treat the valence electrons of H, Au, Ti and O atoms with the reference configurations  $1s^1 2p^0 3d^0 4f^0$  for H,  $6s^1 6p^0 5d^{10} 5f^0$  for Au,  $4s^2 4p^0 3d^2 4f^0$  for Ti,

and  $2s^2 2p^4 3d^0 4f^0$  for O. Double- $\zeta$  plus polarization function (DZP) basis sets are used for Au, Ti and O, and triple- $\zeta$  plus polarization function (TZP) for H. The remaining core electrons are represented by the Troullier-Martins norm-conserving pseudopotentials<sup>56</sup> in the Kleinman-Bylander factorised form.<sup>57</sup> Relativistic effects are taken into account for Au.

Calculations have been carried out with the use of the SIESTA code.<sup>58–60</sup> Periodic boundary conditions are used for all systems, including free molecules and clusters. In the latter case the size of a supercell was chosen to be large enough to make intermolecular interactions negligible.

Within the SIESTA approach, the basis functions and the electron density are projected onto a uniform real-space grid. The mesh size of the grid is controlled by an energy cutoff, which defines the wavelength of the shortest plane wave that can be represented on the grid. In the present work the energy cutoff of 200 Ry is chosen to guarantee convergence of the total energies and forces. The self-consistency of the density matrix is achieved with a tolerance of  $10^{-4}$ . For geometry optimization the conjugate-gradient approach was used with a threshold of  $0.02 \text{ eV \AA}^{-1}$ .

The range of the basis pseudoatomic orbitals (PAO) is limited by an energy shift parameter which defines the confinement of the basis functions. It has been shown that systematic convergence to physical quantities can be obtained by varying the energy shift.<sup>54,55</sup> A common energy shift of 50 meV is applied for Au, Ti and O on the basis of careful comparison of the obtained theoretical results with the available reference data for the free  $\text{Au}_2$  dimer, small gold clusters, bulk Au and  $\text{TiO}_2$ . Thus the calculated values of the dissociation energy and bond length in  $\text{Au}_2$  (2.29 eV, 2.572 Å) are in an excellent agreement with those of earlier experimental studies, (2.31 eV, 2.472 Å).<sup>61</sup> The optimized lattice constant of the face-centered cubic (fcc) structure of bulk gold is 4.208 Å, which is 3% larger than the experimental value of 4.079 Å.<sup>62</sup> This is a general feature of PBE functional to overestimate the lattice constants for various types of solids.<sup>63</sup> In addition we tested the ability of our approach to reproduce the optimized structures and isomer sequences of small free gold clusters consisting of up to 10 atoms. The obtained structures are in a good agreement with those reported in our recent work ref. 24 and previous theoretical studies; see, e.g., refs. 64–68.

Basis set for hydrogen was optimized with the use of the Nelder-Mead simplex method<sup>69</sup> according to the procedure described in ref. 55. The dissociation energy,  $D_e$ , and bond length in  $\text{H}_2$  (4.55 eV, 0.750 Å) are in a good agreement with experimental data (4.74 eV, 0.741 Å).<sup>61</sup> We also tested the gold – hydrogen interaction optimizing AuH dimer. The calculated dissociation energy and bond

length in AuH (3.09 eV, 1.547 Å) are in a good agreement with experimental data (3.36 eV, 1.524 Å).<sup>61</sup>

The rutile structure belongs to the  $P4_2/mnm$  tetragonal space group. The primitive unit cell contains two  $\text{TiO}_2$  units. The unit cell parameters determined by neutron diffraction are found to be  $a=b=4.587$  Å,  $c=2.954$  Å at 15 K.<sup>70,71</sup> In the present work the rutile lattice was optimized using the Monkhorst-Pack<sup>72</sup>  $6\times 6\times 9$  k-point mesh for Brillouin zone sampling. The calculated lattice parameters  $a=4.594$  Å and  $c=2.959$  Å are in excellent agreement with the experimental values.

The optimized lattice of the bulk rutile was used to construct slabs for the  $\text{TiO}_2(110)$  surface. The six-layer slab containing four units of  $\text{TiO}_2$  represents the element of the (110) rutile face with the surface area of  $\sqrt{2}a\times c$ . In the present work we study adsorption of  $\text{Au}_n$  clusters containing  $n = 1, 2, 8$  and 20 atoms on the rutile (110) surface. In the case of Au and  $\text{Au}_2$  the  $\text{TiO}_2(110)$  surface is modeled by the  $p(2\times 5)$  slab (40 units of  $\text{TiO}_2$  per slab), while for  $\text{Au}_8$  and  $\text{Au}_{20}$  we use  $p(3\times 6)$  (72 units of  $\text{TiO}_2$ ) and  $p(4\times 9)$  (144 units of  $\text{TiO}_2$ ) slabs, respectively. The periodically replicated slabs are separated by the vacuum region of 25 Å in the (110) direction. It has been shown that the surface energy, the energy gap and interlayer distances in thin films of rutile oscillate with decreasing amplitude as the number of layers increases.<sup>73–75</sup> The choice of the six-layer slab provides good convergence of the obtained results at moderate computational cost. Similar slab model has been used in ref. 76 to study an  $\text{O}_2$  supply pathways in CO oxidation on Au/ $\text{TiO}_2(110)$ .

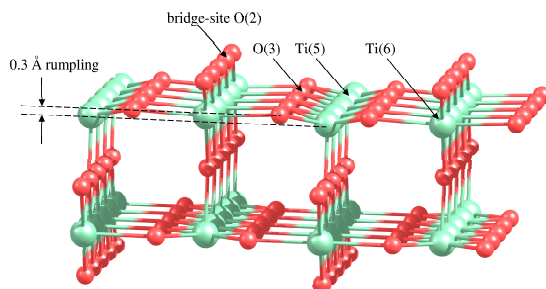


Figure 1: Side view of the  $\text{TiO}_2(110)$   $p(2\times 5)$  slab. The bridge-site twofold coordinated O(2) atom, threefold coordinated O(3) atom, five- and sixfold coordinated Ti(5) and Ti(6) atoms are marked, respectively. Relaxation of the  $\text{TiO}_2(110)$  surface results in a surface rumpling.

Fig. 1 presents the side view of the  $\text{TiO}_2(110)$   $p(2 \times 5)$  slab. The  $\text{TiO}_2(110)$  surface contains atoms with different coordination. The fivefold coordinated Ti atoms are undercoordinated relatively to the bulk sixfold coordinated Ti. The O atoms raised above the plane of Ti atoms are twofold coordinated. These atoms are called bridge-site O. The oxygen atoms lying in the plane of Ti atoms are threefold coordinated. In all calculations the bottom two layers in the slabs are fixed, and all other atoms are fully relaxed. Relaxation of the  $\text{TiO}_2(110)$  surface results in a surface rumpling, as it is shown in Fig. 1. The undercoordinated Ti and O atoms are moving inward by  $0.10 \text{ \AA}$ , decreasing the distance with subsurface atoms. The sixfold coordinated Ti atoms and threefold coordinated O atoms are moving outward by  $0.1 \text{ \AA}$  and  $0.2 \text{ \AA}$ , respectively. The similar puckered structure of the rutile (110) surface has been reported in refs. 73,75.

## 3 Results

### 3.1 Hydrogen adsorption on free gold clusters

The molecular and dissociative adsorption of  $\text{H}_2$  on the free gold clusters of different sizes, chains of gold atoms, and extended gold surfaces have been the subject of a number of theoretical studies.<sup>40,41,43,46,77-79</sup> It was demonstrated that  $\text{H}_2$  effectively adsorbs and dissociates at the low coordinated Au atoms regardless if they are in gold clusters or at extended line defects, such as monoatomic rows on Au surface.<sup>43,46</sup> However, in the case of small Au clusters, coordination alone cannot explain all the features of the reactivity of gold clusters for  $\text{H}_2$  dissociation.<sup>79</sup> Several major factors are determining the catalytic properties of free clusters: the structure associated with individual atoms (i.e. coordination), the binding structure, and the border effects.<sup>79</sup> It was demonstrated that the planar gold structures are not reactive, when the  $\text{H}_2$  approaches the cluster from the top. However, dissociation of  $\text{H}_2$  can be promoted when planar clusters are folded or the  $\text{H}_2$  approaches clusters in their plane.<sup>79</sup> The flexibility can play an important role in  $\text{H}_2$  dissociation, because of the large atomic displacements in the cluster.<sup>43</sup> Finally, the size, the structure and the charge state of gold clusters influence on the molecular and dissociative adsorption of  $\text{H}_2$ .<sup>78</sup>

In the present work we consider adsorption of  $\text{H}_2$  on gold clusters  $\text{Au}_n$  consisting of  $n = 1, 2, 8,$  and  $20$  atoms in order to elucidate the size and the geometry effects on hydrogen adsorption. The structural properties of free gold clusters have been intensively studied, see, e.g., refs. 19,68,80 for a review. DFT calcula-

tions demonstrate that  $\text{Au}_n$  clusters favor planar, two-dimensional (2D) structures up to cluster size of 11-13 atoms, while  $\text{Au}_n$  of larger sizes are three-dimensional (3D).<sup>67,81,82</sup> The high stability of planar structures for small gold clusters has been explained by relativistic effects. The relativistic effects make the  $6s$  and  $5d$  atomic orbitals closer in energy, resulting in a  $sd$  hybridization, which in turn stabilizes planar configurations.<sup>83</sup> The exact value of the critical size for  $2\text{D} \rightarrow 3\text{D}$  transition in neutral  $\text{Au}_n$  is not yet clarified. *Ab initio* MP2 and CCSD(T) calculations performed in ref. 84 demonstrate that  $\text{Au}_8$  possesses 3D structure, while the similar CCSD(T) calculations performed with the larger basis set favors 2D structure for  $\text{Au}_8$ .<sup>85</sup> Recent CCSD(T) calculations accounting for the basis-set superposition error (BSSE) corrections are in favor of 3D structure for  $\text{Au}_{10}$ <sup>86</sup> in accord with DFT predictions. Competition of 2D and 3D structures of the small gold clusters is a very interesting feature that can play an important role in cluster reactivity. The 2D structures contain a large number of low coordinated atoms, hence they might possess higher catalytic activity in comparison with the 3D clusters. Moreover, it has been shown that if the shape of neutral gold clusters is modified, it is possible to change their electron donor-acceptor capacities – the 2D gold clusters are better electron acceptors than 3D ones.<sup>87</sup> Since the electron transfer between the cluster and the adsorbate is an important driving force for the reactivity, the shape of the cluster can directly affect cluster’s catalytic properties.<sup>87</sup>

In our previous works we have optimized the most stable and isomer geometries of small gold clusters consisting up to 10 atoms within DFT B3PW91/LANL2DZ approach.<sup>9,24</sup> In the present work we have re-optimized the earlier obtained geometries of  $\text{Au}_n$  using the PBE/DZP SIESTA method. The obtained structures are in an excellent agreement with those reported in previous theoretical studies; see, e.g., refs. 24,64–68.

In Fig. 2 we present optimized geometries of  $\text{H}_2 - \text{Au}_n$  systems in the case of molecular and dissociative adsorption of  $\text{H}_2$  on free  $\text{Au}_n$  clusters. In order to obtain the most stable configuration of  $\text{H}_2$  adsorbed on  $\text{Au}_n$ , we have created a large number of starting geometries by adding  $\text{H}_2$  molecule in different positions (up to 30) on the surface of the considered clusters. The starting structures have been optimized further without any geometry constraints. We have successfully used a similar approach to find the optimized geometries of  $\text{O}_2$  and  $\text{C}_2\text{H}_4$  molecules adsorbed on small neutral, anionic and cationic gold clusters.<sup>9,10,24,88</sup> In addition to the most stable 2D structure of  $\text{Au}_8$  and 3D structure of  $\text{Au}_{20}$  we consider the closest in energy 3D isomer of  $\text{Au}_8$  and 2D isomer of  $\text{Au}_{20}$  in order to understand how dimensionality and structural properties affect the cluster reactivity. The calculated relative energies for the higher isomeric  $\text{Au}_8$  (3D) and  $\text{Au}_{20}$  (2D)



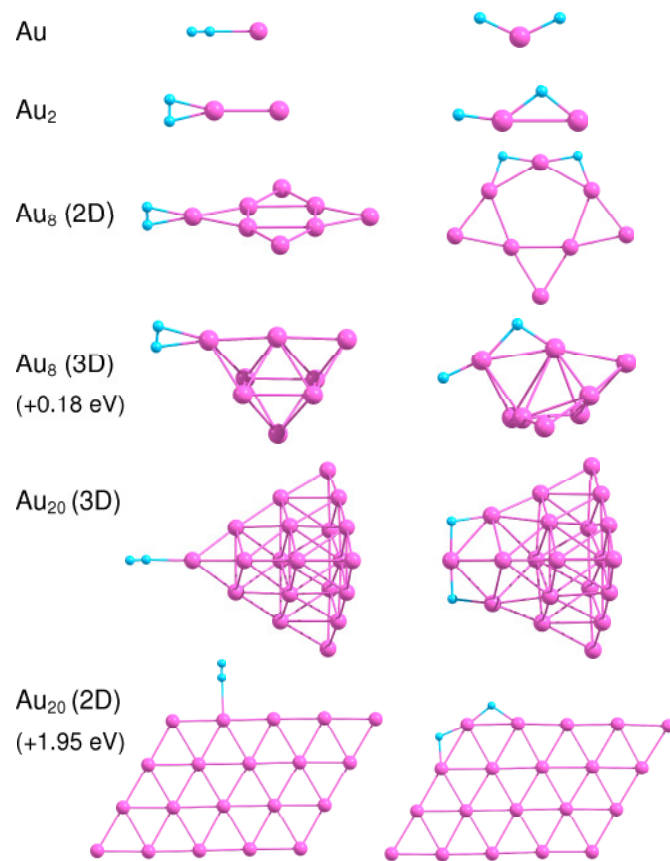


Figure 2: Optimized geometries of  $H_2-Au_n$  clusters in the case of molecular (left) and dissociative (right) adsorption of  $H_2$ . The numbers in the parentheses correspond to the relative energy for the higher isomeric free  $Au_8$  (3D) and  $Au_{20}$  (2D) clusters with respect to the corresponding  $Au_8$  (2D) and  $Au_{20}$  (3D) lowest energy structures.

structures with respect to the corresponding lowest energy structures are 0.18 eV and 1.95 eV, respectively. The binding energies for molecular,  $E_b^{mol}$ , and dissociative,  $E_b^{dis}$ , adsorption of  $H_2$  on free  $Au_n$  as well as the H–H bond length  $r_{H-H}^{mol}$  in  $H_2$  adsorbed molecularly are summarized in Table 1.

Table 1: Binding energies for molecular,  $E_b^{mol}$ , and dissociative,  $E_b^{dis}$ , adsorption of  $H_2$  on free  $Au_n$  clusters and the H–H bond length,  $r_{H-H}^{mol}$ , in the case of molecular adsorption of  $H_2$ .

Cluster	$r_{H-H}^{mol}$ (Å)	$E_b^{mol}$ (eV)	$E_b^{dis}$ (eV)
Au	0.780	0.13	0.04
Au <sub>2</sub>	0.845	0.59	0.59
Au <sub>8</sub> (2D)	0.806	0.26	0.68
Au <sub>8</sub> (3D)	0.788	0.13	0.52
Au <sub>20</sub> (3D)	0.768	0.09	0.14
Au <sub>20</sub> (2D)	0.762	0.09	0.72

The binding energy of  $H_2$  adsorbed on a free  $Au_n$  cluster is defined as

$$E_b^{mol,dis} = E_{tot}(Au_n) + E_{tot}(H_2) - E_{tot}^{mol,dis}(H_2-Au_n), \quad (1)$$

where  $E_{tot}^{mol,dis}(H_2-Au_n)$  denotes the total energy of the compound system,  $H_2-Au_n$ , while  $E_{tot}(Au_n)$  and  $E_{tot}(H_2)$  are the total energies of the non-interacting fragments  $Au_n$  and  $H_2$ , respectively.

Results of our calculations demonstrate, that  $H_2$  binds weakly to Au as a molecule, with  $E_b^{mol}=0.13$  eV. Dissociation of  $H_2$  on Au is not favorable energetically. The H–H bond length in  $H_2$  adsorbed on Au is slightly enlarged in comparison with the free  $H_2$ . Adsorption of  $H_2$  on  $Au_2$  is relatively strong, with the binding energy equal to 0.59 eV both for the molecular and the dissociative adsorption. Table 1 demonstrates that the H–H bond length increases to 0.845 Å in  $H_2-Au_2$ , indicating that  $H_2$  is highly activated.

With the further increase in cluster size the binding energy calculated for molecular adsorption of  $H_2$  decreases to 0.26 eV (0.13eV) for  $Au_8$  (2D) ( $Au_8$  (3D)) and 0.09 eV both for 3D and 2D isomers of  $Au_{20}$ . On the other hand, the dissociative adsorption of  $H_2$  becomes energetically favorable both for  $Au_8$  and  $Au_{20}$ . The binding energy of  $H_2$  on free gold clusters strongly depends on the cluster’s isomer state. Thus, dissociative adsorption of  $H_2$  on 2D structures of  $Au_8$  and  $Au_{20}$  are energetically favorable compared with the corresponding 3D structures. Therefore, dissociation of  $H_2$  on small gold clusters can be promoted

if we can find a way to enhance the stability of 2D structures for  $n \geq 13$ . That should be possible for supported clusters, where an attractive interaction with the surface stabilizes oblate configurations.<sup>89</sup> Thus, varying the interaction with the support one can change the cluster shape, and hence it can be possible to tune its reactivity. Another factors that influence  $H_2$  dissociation are coordination of Au atoms interacting with hydrogen and flexibility of cluster structure. It is seen from Fig. 2 that  $H_2$  dissociates at the low coordinated corner Au atom with formation of the slightly bended H–Au–H bond. It is worth to note, that the Au–Au bond length in  $Au_2$  does not change noticeably upon molecular adsorption of  $H_2$ ; but increases up to 2.753 Å for dissociative adsorption. In the case of  $Au_8$  and  $Au_{20}$  dissociation of  $H_2$  on the cluster surface is accompanied by the structural (at least local) transformations. Therefore we can confirm conclusion made in ref. 43 that the structural flexibility of the gold clusters might be an important factor for  $H_2$  dissociation.

### 3.2 Hydrogen adsorption on $Au_n/TiO_2(110)$

How does the interaction with the support influence the reactivity of gold clusters? Can a supported nanoparticle exhibit novel properties that are not found for free particles? Recent experiments performed by Haruta *et al* clearly demonstrate that the perimeter interface of the gold nanoparticles supported on the rutile  $TiO_2(110)$  surface plays a crucial role in the process of hydrogen dissociation.<sup>37</sup> It was suggested that the active sites for  $H_2$  dissociation might be formed by a combination of gold atoms and oxygen atoms from  $TiO_2$  at the nanoparticle–surface interface.<sup>37</sup>

In the present work we perform a systematic theoretical study of the structure and energetics of  $H_2$  adsorbed on  $Au_1$ ,  $Au_2$ ,  $Au_8$  (2D),  $Au_8$  (3D),  $Au_{20}$  (3D) and  $Au_{20}$  (2D) clusters supported on the rutile  $TiO_2(110)$  surface. The analysis of the energetics of  $H_2$  adsorption on the supported gold clusters provides deep insights into the nature of bonding and dissociation of the  $H_2$  molecule and reveals the details of the reaction mechanism.

As discussed above the dissociation of  $H_2$  on free gold clusters is governed by the interplay of structural factors, coordination of the adsorption center and cluster flexibility. The complexity of the changes in structural and electronic features of gold nanoparticles becomes more diverse when one deposit nanoparticle on the support.

In order to obtain the most stable geometries of  $Au_n$  supported on the rutile  $TiO_2(110)$  surface we have created a large number of starting configurations by

adding  $Au_n$  isomers with different orientation in respect to the surface. These structures have been fully optimized on the rutile surface, with accounting for the relaxation of all the gold atoms as well as the top four layers of the six layer slab of the rutile. The bottom two layers in the slab were fixed. Thus, we have taken into account deformations of the cluster structure due to the interaction with the support as well as structural relaxations on the rutile  $TiO_2(110)$  surface due to its interaction with the supported cluster.

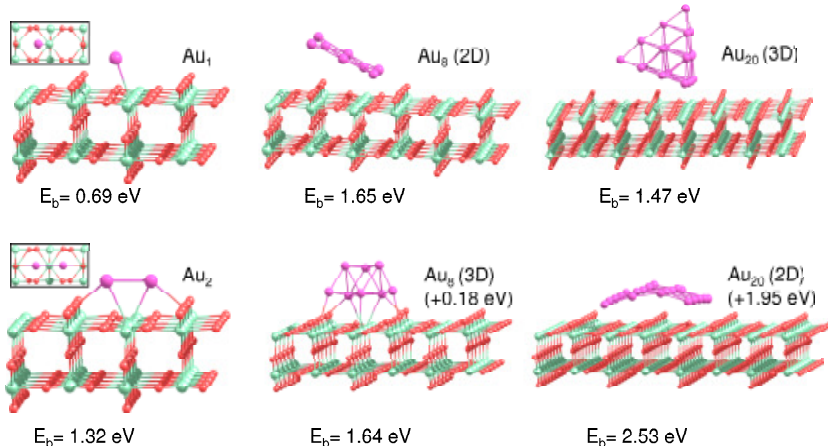


Figure 3: The most stable geometries of  $Au_n$  clusters ( $n = 1, 2, 8,$  and  $20$ ) optimized on the rutile  $TiO_2(110)$  surface. Top views of  $Au$  and  $Au_2$  on  $TiO_2(110)$  are shown in the inserts. The binding energies of  $Au_n$  on  $TiO_2(110)$  are marked below the corresponding structures. Numbers in parentheses correspond to the relative energy for the higher isomeric free  $Au_8$  (3D) and  $Au_{20}$  (2D) clusters with respect to the corresponding free  $Au_8$  (2D) and  $Au_{20}$  (3D) lowest energy structures.

Fig. 3 presents the most stable geometries of  $Au_n$  clusters ( $n = 1, 2, 8,$  and  $20$ ) optimized on the rutile  $TiO_2(110)$  surface. We found that gold tends to maximize interaction with the O(3) and Ti(5) atoms on  $TiO_2(110)$  surface. Thus, Au atom tends to occupy a position above the row of O(3) surface atoms, simultaneously bridging two O(3) atoms in the direction parallel to the O(3) row, as well as Ti(5) and O(2) atoms, in the direction perpendicular to the O(3) row. In the case of  $Au_2$ ,

both of Au atoms occupy positions above of the rows of O(3) atoms, symmetrically in respect to the row of Ti(5) atoms. The Au–Au bond length of 2.57 Å in Au<sub>2</sub> matches the distance between the two rows of O(3) atoms (2.53 Å). The geometry structures of two- and three dimensional isomers of Au<sub>8</sub> on the TiO<sub>2</sub>(110) surface are slightly deformed if compared with the free gold clusters. The Au<sub>8</sub> (2D) cluster maximizes the interaction between the cluster edge and the row of O(3) atoms on the TiO<sub>2</sub>(110) surface. The angle between the cluster’s plane and the rutile surface is 26°. The supported Au<sub>8</sub> (3D) isomer prefers to maximize its interaction with the rutile TiO<sub>2</sub>(110) surface, orienting the 5-atom face parallel to the support, as shown in Fig. 3. The binding energies of Au<sub>8</sub> (2D) and Au<sub>8</sub> (3D) isomers on TiO<sub>2</sub>(110) are 1.65 eV and 1.64 eV, respectively. A tetrahedral Au<sub>20</sub> (3D) cluster binds to the surface, maximizing interaction between the cluster edge and rows of O(3) and Ti(5) surface atoms; while Au<sub>20</sub> (2D) isomer binds by two its edges to two parallel rows of Ti(5) surface atoms, slightly bending its planar structure, to avoid interaction with the row of O(2) bridge atoms in the middle. The planar Au<sub>20</sub> structure binds to the surface much more strongly than the 3D structure, because it has a wider contact area. Although Au<sub>20</sub> (3D) structure is still energetically favorable when adsorbed on the TiO<sub>2</sub>(110) surface in comparison with the 2D structure, the energy difference between two configurations decreases from 1.95 eV for free clusters to 0.89 eV for supported clusters, respectively. If we could further increase the interaction with the support, we would make 2D structure energetically favorable. Such an effect has been reported for Au<sub>20</sub> clusters deposited on thin MgO(100) films supported on Mo(100) substrate.<sup>90</sup> By changing the thickness of the metal-oxide film, one can tune the interaction of the cluster with the support, and thus increase its wetting propensity and induce a dimensionality crossover from 3D cluster structures on MgO(100) to the energetically favored 2D geometries on the metal-supported films.<sup>90</sup>

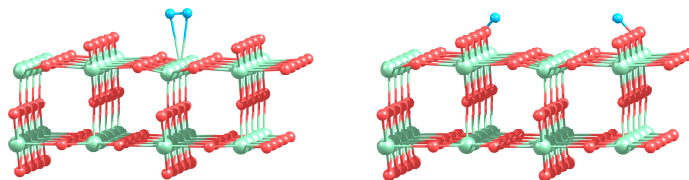


Figure 4: Optimized geometries for molecular (left) and dissociative (right) adsorption of H<sub>2</sub> on the pure rutile TiO<sub>2</sub>(110) surface.

Fig. 4 presents the most stable geometries calculated for the molecular and dissociative adsorption of  $H_2$  on the pure rutile  $TiO_2(110)$  surface. Our calculations demonstrate that the hydrogen molecule adsorbs on the pure rutile  $TiO_2(110)$  surface on top of the Ti(5) atom with the binding energy of 0.14 eV. The H–H bond length of 0.78 Å is slightly increased in comparison with the free  $H_2$ . The dissociative state of  $H_2$  on  $TiO_2(110)$  corresponds to the situation when both H atoms form the OH group with the low coordinated O(2) bridge atoms on the rutile surface. The binding energy of the dissociated configuration of  $H_2$  is 1.50 eV; however, the distance between two rows of O(2) atoms on  $TiO_2(110)$  is 6.50 Å, which is too large to promote dissociation of the  $H_2$  adsorbed on top of Ti(5) atom. In this case  $H_2$  would dissociate in the vicinity of the adsorption center as a first step, followed by adsorption of H atoms on O(2). This process would require to overcome a dissociation barrier much higher than the energy of the molecular adsorption. In this situation  $H_2$  would likely desorb from the surface and fly away rather than dissociate. Therefore, to promote  $H_2$  dissociation on  $TiO_2(110)$ , it is necessary to have adsorption centers on the rutile surface in the vicinity of low coordinated O(2) atoms. Supported gold clusters can serve as a source of such centers.

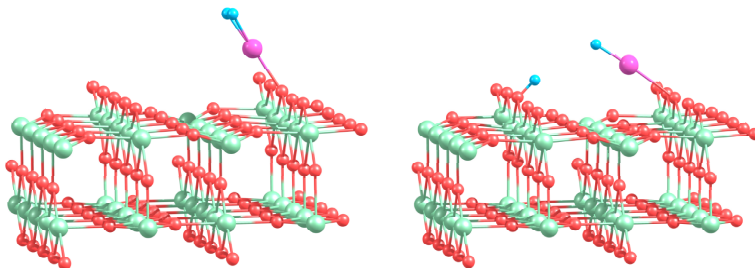


Figure 5: Optimized geometries for molecular (left) and dissociative (right) adsorption of  $H_2$  on  $Au/TiO_2$ .

Fig. 5 presents optimized geometries calculated for molecular and dissociative adsorption of  $H_2$  on  $Au/TiO_2$ . It is seen from Table 2 that  $H_2$  adsorbs molecularly on  $Au/TiO_2$  with a binding energy of 1.15 eV, which is considerably larger than the corresponding energy calculated for  $H_2$  adsorbed on free Au atom. The adsorbed  $H_2$  is highly activated, with the H–H bond length  $r_{H-H}^{mol}=0.906$  Å. As a result of  $H_2$  adsorption, the supported Au atom shifts slightly towards the row of the low coordinated O(2) bridge atoms. In the previous section we saw that

Table 2: Binding energy calculated for molecular,  $E_b^{mol}$ , and dissociative,  $E_b^{dis}$ , adsorption of  $H_2$  on  $Au_n/TiO_2$ , and the H–H bond length,  $r_{H-H}^{mol}$ , in the case of molecular adsorption of  $H_2$ .

Cluster	$r_{H-H}^{mol}$ (Å)	$E_b^{mol}$ (eV)		$E_b^{dis}$ (eV)	
Au	0.906	1.15		2.06	
Au <sub>2</sub>	0.821	0.37		0.73 <sup>(b)</sup>	0.90 <sup>(c)</sup> 1.55 <sup>(d)</sup>
Au <sub>8</sub> (2D)	0.792	0.24		0.75 <sup>(b)</sup>	1.55 <sup>(c)</sup>
Au <sub>8</sub> (3D)	0.753	0.09		0.55 <sup>(e)</sup>	0.95 <sup>(f)</sup>
Au <sub>20</sub> (3D)	0.795 <sup>(a)</sup> 0.806 <sup>(a')</sup>	0.17 <sup>(a)</sup>	0.13 <sup>(a')</sup>	0.20 <sup>(b)</sup>	0.83 <sup>(c)</sup>
Au <sub>20</sub> (2D)	0.798 <sup>(d)</sup> 0.805 <sup>(d')</sup>	0.11 <sup>(d)</sup>	0.11 <sup>(d')</sup>	0.55 <sup>(e)</sup>	1.42 <sup>(f)</sup>

$H_2$  dissociation is not favorable on the free Au atom. However, in the case of the supported Au atom, dissociation of  $H_2$  can occur with formation of the OH group with the O(2) atom located either in the nearest to Au row of O(2) or in the next row of O(2), as is shown in Fig. 5. In the latter case the calculated binding energy  $E_b^{dis}=2.06$  eV is higher, not only if compared with the binding energy for molecular adsorption of  $H_2$  on  $Au/TiO_2(110)$ , but also if compared with the binding energy of the dissociated state of  $H_2$  on the pure  $TiO_2(110)$  surface. Thus, we can conclude, from the energetic point of view, that the  $TiO_2(110)$  support considerably promotes  $H_2$  dissociation on Au atom.

The optimized geometries calculated for molecular and dissociative adsorption of  $H_2$  on  $Au_2/TiO_2$  are shown in Fig. 6. Figs. 6(a) and 6(b) demonstrate that  $H_2$  binds to the supported  $Au_2$  in a similar way as for the free  $Au_2$ . However the binding energy calculated for the molecular adsorption of  $H_2$  on  $Au_2/TiO_2$  is lower than the corresponding energy obtained for free  $Au_2$ , while the dissociated configuration of  $H_2$  on  $Au_2/TiO_2$  is more stable if compared with dissociative adsorption of  $H_2$  on the free  $Au_2$ . Therefore, the interaction of  $Au_2$  with the support results in the energetic promotion of  $H_2$  dissociation on the supported  $Au_2$ . We found, however, that the geometry configuration shown in Fig. 6(b) is not the most stable one for  $H_2$  dissociation. We found that the hydrogen atom can migrate to the row of O(3) atoms, or to the row of O(2) bridge atoms on the rutile surface, forming OH bonds, as it is shown in Figs. 6(c) and 6(d), respectively. Hydrogen atom always binds more strongly with the low coordinated O(2) atoms, as can be seen from Table 2.

Figs. 7(a), 7(b), 7(d) and 7(e) demonstrate that optimized geometries of  $H_2$  in the case of its molecular and dissociative adsorption on the supported  $Au_8$  (2D)

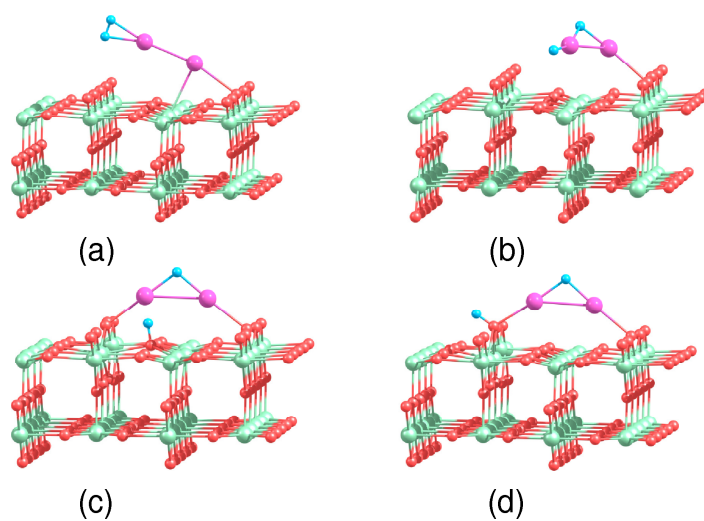


Figure 6: (a) Optimized geometry in the case of molecular adsorption of H<sub>2</sub> on Au<sub>2</sub>/TiO<sub>2</sub>. Optimized geometries in the case of dissociative adsorption of H<sub>2</sub> on Au<sub>2</sub>/TiO<sub>2</sub>: (b) dissociation of H<sub>2</sub> on supported Au<sub>2</sub>; (c) dissociation of H<sub>2</sub> with formation of the OH group on O(3) surface atom; (d) dissociation of H<sub>2</sub> with formation of the OH group on O(2) bridge atom.



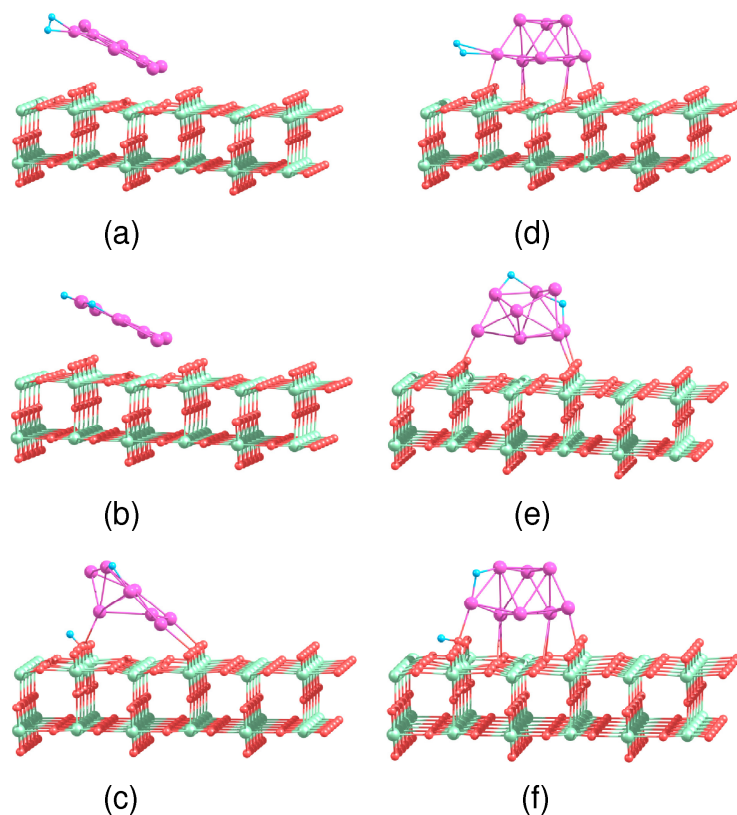


Figure 7: Optimized geometries in the case of (a) molecular adsorption of  $\text{H}_2$  on  $\text{Au}_8(2\text{D})/\text{TiO}_2$ ; dissociative adsorption of  $\text{H}_2$  on  $\text{Au}_2(2\text{D})/\text{TiO}_2$ : (b) dissociation of  $\text{H}_2$  on supported  $\text{Au}_2(2\text{D})$ ; (c) dissociation of  $\text{H}_2$  with formation of the OH group on O(2) bridge atom. Optimized geometries in the case of (d) molecular adsorption of  $\text{H}_2$  on  $\text{Au}_8(3\text{D})/\text{TiO}_2$ ; dissociative adsorption of  $\text{H}_2$  on  $\text{Au}_2(3\text{D})/\text{TiO}_2$ : (e) dissociation of  $\text{H}_2$  on supported  $\text{Au}_2(3\text{D})$ ; (f) dissociation of  $\text{H}_2$  with formation of the OH group on O(2) bridge atom.

and Au<sub>8</sub> (3D) clusters similar to those obtained for the corresponding free Au<sub>8</sub> clusters. Note that the dissociative adsorption of H<sub>2</sub> on Au<sub>8</sub> (3D) results in the considerable rearrangement of the gold structure as shown in Fig. 7(e). Tables 1 and 2 demonstrate that the binding energies calculated for molecular adsorption of H<sub>2</sub> on free and supported Au<sub>8</sub> (2D) and Au<sub>8</sub> (3D) are quite similar. However, the dissociative configuration of H<sub>2</sub> on the supported Au<sub>8</sub> (2D) and Au<sub>8</sub> (3D) clusters is slightly promoted energetically. Migration of H on the low coordinated O(2) atom as it is shown in Figs. 7(c) and 7(f), results in formation of the OH bond and considerable increase in binding energies calculated for H<sub>2</sub> adsorbed dissociatively. It is seen from Fig. 7(c) that the planar structure of Au<sub>8</sub> undergoes drastic rearrangements upon H<sub>2</sub> dissociation. The dissociative adsorption of H<sub>2</sub> on Au<sub>8</sub> is energetically favorable if compared with the adsorption on the 3D isomer of Au<sub>8</sub>.

The Au<sub>20</sub> (3D) and Au<sub>20</sub> (2D) clusters supported on TiO<sub>2</sub>(110) are the largest systems studied in the present work. In the previous section it was shown that the hydrogen molecule binds weakly to the free Au<sub>20</sub> (3D) and Au<sub>20</sub> (2D) clusters. We have found that, in the case of the supported Au<sub>20</sub>, the hydrogen molecule adsorbs on top of the Ti(5) atoms on the rutile surface in the vicinity of Au<sub>20</sub>, rather than directly on the Au<sub>20</sub> clusters, as it is shown in Figs. 8(a), 8(d) and 8(d'). The geometry structure when H<sub>2</sub> adsorbs at the vertex of Au<sub>20</sub>(3D), bridging Au vertex atom in the cluster and the low coordinated O(2) atom on the rutile surface is also stable (Fig. 8(a')). Further H<sub>2</sub> dissociation can occur either at the vertex of Au<sub>20</sub> (3D) or at the acute-angled corner of Au<sub>20</sub> (2D), as is shown in Fig. 8(b) and Fig. 8(e), respectively. H<sub>2</sub> dissociation at the acute-angled corner of Au<sub>20</sub> (2D) is accompanied by severe local structural rearrangement of Au atoms at the corner of Au<sub>20</sub> (2D) and migration of one H atom to the O(2) atom on the surface. Note that the dissociation of H<sub>2</sub> at the obtuse-angled corner of the supported Au<sub>20</sub> (2D) cluster is not energetically favorable, in comparison to the case of free Au<sub>20</sub> (2D). The most stable configurations of the dissociated H<sub>2</sub> are those where one of the H atoms binds to the edges of Au<sub>20</sub> (3D) or Au<sub>20</sub> (2D) that are oriented perpendicularly to the rows of O(2) surface atoms, while another H forms the OH bond with the O(2) atom on the rutile surface, as is shown in Figs. 8(c) and 8(f). We found several geometrical configurations of this type with binding energies of 1.19 - 1.42 eV. Dissociation at the edge of the supported 2D isomer of Au<sub>20</sub> is always energetically favorable.

Thus, combination (interplay) of several factors such as geometry structure, cluster dimensionality, presence of the low coordinated oxygen atoms in the vicinity of the cluster-surface interface, etc. are important for H<sub>2</sub> dissociation.

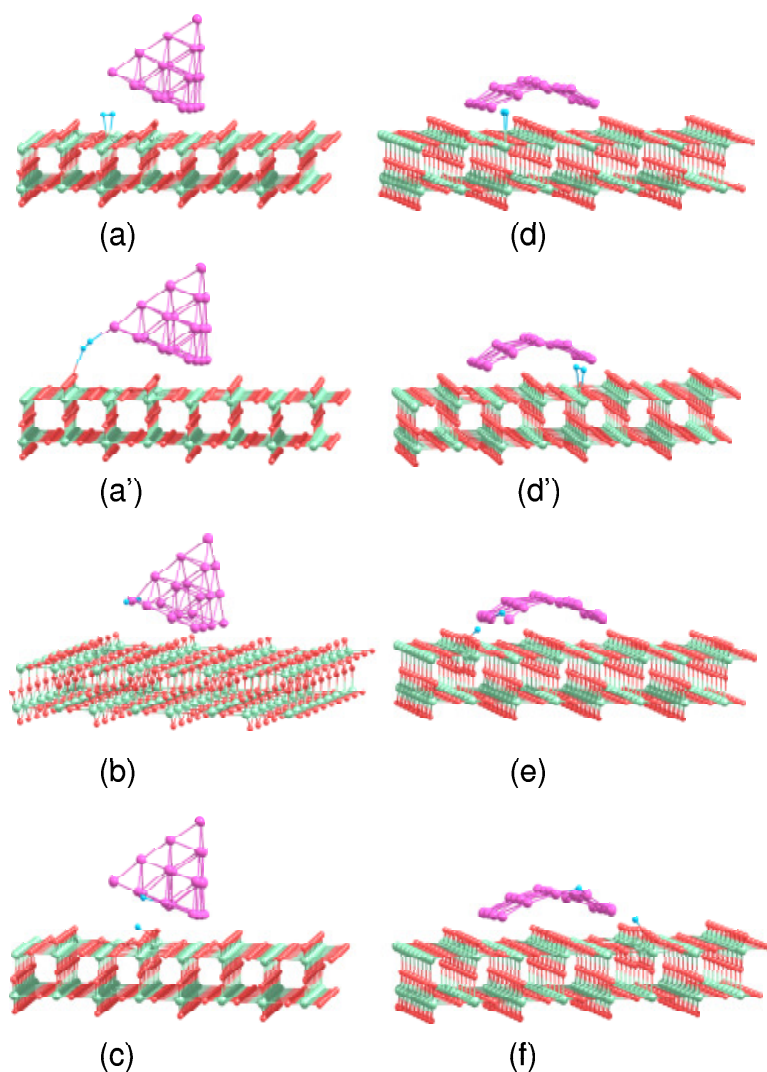


Figure 8: Optimized geometries for  $\text{H}_2$  adsorbed on  $\text{Au}_{20}(3\text{D})/\text{TiO}_2$  (left) and  $\text{Au}_{20}(2\text{D})/\text{TiO}_2$  (right). (a) and (a') Molecular adsorption of  $\text{H}_2$  in the vicinity of  $\text{Au}_{20}(3\text{D})/\text{TiO}_2$ ; (b) dissociative adsorption of  $\text{H}_2$  at the vertex of  $\text{Au}_{20}(3\text{D})$  with formation of the OH group; (c) dissociative adsorption of  $\text{H}_2$  at edge of  $\text{Au}_{20}(3\text{D})$  with formation of the OH group; (d) and (d') molecular adsorption of  $\text{H}_2$  in the vicinity of  $\text{Au}_{20}(2\text{D})/\text{TiO}_2$ ; (e) dissociative adsorption of  $\text{H}_2$  at the corner of  $\text{Au}_{20}(2\text{D})$  with formation of the OH group; (f) dissociative adsorption of  $\text{H}_2$  at edge of  $\text{Au}_{20}(2\text{D})$  with formation of the OH group.

It is well known that, in the case of catalytic oxidation reactions by molecular oxygen on free and supported gold nanoparticles, the charge transfer from the gold to the antibonding orbital of  $O_2$  is responsible for the catalytic activation and dissociation of  $O_2$ . However, in the case of  $H_2$  dissociation the analysis of the Bader charges<sup>91,92</sup> demonstrate that there is no considerable charge transfer between the adsorbed hydrogen and the gold clusters (free or supported). We found the largest charge transfer occurs for  $H_2$  adsorbed molecularly on Au/TiO<sub>2</sub> (Fig. 5). In this case the calculated Bader charge localized on  $H_2$  is +0.11e, where e is the elementary charge. Although such a charge transfer is relatively small, it might be responsible for the strong enlargement of the H–H bond length in  $H_2$ –Au/TiO<sub>2</sub> up to 0.906 Å. Nevertheless, we have not found the direct correlation of the hydrogen dissociation with the charge transfer between hydrogen and gold atoms. On the other hand, formation of the OH group with the bridge O(2) atom on the rutile surface is accompanied by the large charge transfer from H atom to O(2), resulting in a Bader net charge of H in OH equal to +0.75e. Thus, we can conclude that the catalytic activity of gold nanoparticles for  $O_2$  dissociation would depend on the electronic structure and the size of the nanoparticles; however in the case of  $H_2$  dissociation it will be proportional to the number of gold atoms located in the vicinity of the low coordinated O(2) atoms at the nanoparticle – surface interface.

## 4 Conclusions

The present theoretical study demonstrates that adsorption of  $H_2$  on  $Au_n$  ( $n= 1, 2, 8, 20$ ) strongly depends on cluster size, geometry structure, flexibility and interaction with the support material. Strong interaction with the support can stabilize 2D structures of gold clusters on the surface. This is important finding, because the energy release due to  $H_2$  dissociation is the largest for the 2D isomers of gold clusters. Rutile TiO<sub>2</sub>(110) support energetically promotes  $H_2$  dissociation on gold clusters. The formation of the OH group near the supported gold cluster is an important condition for  $H_2$  dissociation. We have shown that the active sites towards  $H_2$  dissociation on the supported  $Au_n$  are located at corners and edges of the gold cluster in the vicinity of the low coordinated oxygen atoms on TiO<sub>2</sub>(110). Therefore catalytic activity of a gold nanoparticle supported on the rutile TiO<sub>2</sub>(110) surface is proportional to the length of the perimeter interface between the nanoparticle and the support, in accordance with the recent experimental findings.<sup>37</sup>

In the present work we have systematically studied adsorption and dissocia-

tion of H<sub>2</sub> based on the assumption of the total energy criterion. Thus, we have identified a number of the most stable configurations for molecular and dissociative states of H<sub>2</sub> adsorbed on free and supported gold nanoparticles. Conditions leading to the stabilization of the dissociated state of H<sub>2</sub> have been disclosed.

However, many interesting and important questions regarding the mechanism of H<sub>2</sub> dissociation on TiO<sub>2</sub>(110) supported Au<sub>n</sub> clusters remain unanswered. Thus, it is necessary to elucidate the full reaction pathways and to estimate the reaction barriers for H<sub>2</sub> dissociation. This will allow favorable reaction channels and reaction dynamics to be identified. As a next step one should consider simple hydrogenation reactions, such as, for example, hydrogen peroxide formation from H<sub>2</sub> and O<sub>2</sub> catalyzed by the supported gold clusters. We can suggest that structures active for H<sub>2</sub> dissociation, but not active enough for O<sub>2</sub> dissociation could work as catalysts for H<sub>2</sub>O<sub>2</sub> synthesis.

In many cases we have found an ensemble of initial and final configurations of the adsorbed hydrogen with small differences in binding energies, but possible difference in the reaction barriers. Accounting for the geometry of the initial and final states can lead to further non-equivalence of different reaction pathways and may have an important impact on the change of system entropy. It has been argued<sup>93-95</sup> that accounting for an entropy change contribution to the free energy of the system is necessary for correct description of the temperature dependencies of the branching ratios between different reaction channels, while purely energetic considerations based on reaction barrier heights can fail.

Finally, we have considered the pure, defect free rutile TiO<sub>2</sub>(110) surface. It is well known that the surface defects, especially O vacancies in metal-oxide supports, or extra O atoms adsorbed on the surface can change drastically the catalytic activity of the supported gold clusters in oxidation reactions by molecular oxygen.<sup>20,96</sup> Interaction of small gold clusters with a partially reduced rutile TiO<sub>2</sub>(110) support can be rather complicated; supported gold clusters can either receive or donate electrons to the substrate depending on the cluster size.<sup>97</sup> The role of the surface defects in the process of H<sub>2</sub> dissociation is not so obvious and requires additional systematic investigation. Such defects, in particular additional O atoms adsorbed on the surface in the vicinity of the cluster – surface interface can probably play a role in H<sub>2</sub> dissociation and hence can modify the cluster reactivity. Understanding how to control such chemical reactions on a cluster surface is a vital task for nanocatalysis.

We hope that the present discussion will stimulate further experimental and theoretical investigations of the processes considered.

## Acknowledgements

This work was supported by the Global COE Program (Project No. B01: Catalysis as the Basis for Innovation in Materials Science) from the Ministry of Education, Culture, Sports, Science and Technology, Japan; the Grant-in-Aid for the Project on Strategic Utilization of Elements and the JSPS Grant-in-Aid for Scientific Research C. The computations were performed using the Research Center for Computational Science, Okazaki, Japan.

## References

- [1] M. Haruta, T. Kobayashi, H. Sano and N. Yamada, *Chem. Lett.*, 1987, **16**, 405–408.
- [2] M. Haruta, *The Chemical Record*, 2003, **3**, 75–87.
- [3] D. T. Thompson, *Nanotoday*, 2007, **2**, 40–43.
- [4] M. Haruta, *Catalysis Today*, 1997, **36**, 153–166.
- [5] M. Turner, V. B. Golovko, O. P. H. Vaughan, P. Abdulkin, A. Berenguer-Murcia, M. S. Tikhov, B. F. G. Johnson and R. M. Lambert, *Nature*, 2008, **454**, 981–984.
- [6] M. D. Hughes, Y.-J. Xu, P. Jenkins, P. McMorn, P. Landon, D. I. Enache, A. F. Carley, G. A. Attard, G. J. Hutchings, F. King, E. H. Stitt, P. Johnston, K. Griffin and C. J. Kiely, *Nature*, 2005, **437**, 1132–1135.
- [7] H. Tsunoyama, H. Sakurai, Y. Negishi and T. Tsukuda, *J. Am. Chem. Soc.*, 2005, **127**, 9374–9375.
- [8] P. Landon, P. J. Collier, A. J. Papworth, C. J. Kiely and G. Hutchings, *Chem. Commun.*, 2002, 2058–2059.
- [9] A. Lyalin and T. Taketsugu, *J. Phys. Chem. C*, 2009, **113**, 12930–12934.
- [10] A. Lyalin and T. Taketsugu, *J. Phys. Chem. Lett.*, 2010, **1**, 1752–1757.
- [11] A. A. Herzing, C. J. Kiely, A. F. Carley, P. Landon and G. J. Hutchings, *Science*, 2008, **321**, 1331–1335.
- [12] M. J. Rodríguez-Vázquez, M. C. Blanco, R. Lourido, C. Vázquez-Vázquez, E. Pastor, G. A. Planes, J. Rivas and M. A. López-Quintela, *Langmuir*, 2008, **24**, 12690–12694.
- [13] *Nanocatalysis*, ed. U. Heiz and U. Landman, Springer, Berlin, Heidelberg, New York, 2007.
- [14] B. Hvolbæk, T. V. W. Janssens, B. S. Clausen, H. Falsig, C. H. Christensen and J. K. Nørskov, *Nanotoday*, 2007, **2**, 14–18.

- [15] S. M. Lang, T. M. Bernhardt, R. N. Barnett, B. Yoon and U. Landman, *J. Am. Chem. Soc.*, 2009, **131**, 8939–8951.
- [16] U. Landman, B. Yoon, C. Zhang, U. Heiz and M. Arenz, *Topics in Catalysis*, 2007, **44**, 145–158.
- [17] C. Harding, V. Habibpour, S. Kunz, A. N.-S. Farnbacher, U. Heiz, B. Yoon and U. Landman, *J. Am. Chem. Soc.*, 2009, **131**, 538–548.
- [18] J. A. Rodríguez, L. Feria, T. Jirsak, Y. Takahashi, K. Nakamura and F. Illas, *J. Am. Chem. Soc.*, 2010, **132**, 3177–3186.
- [19] R. Coquet, K. L. Howard and D. J. Willock, *Chem. Soc. Rev.*, 2008, **37**, 2046–2076.
- [20] A. Sanchez, S. Abbet, U. Heiz, W.-D. Schneider, H. Hakkinen, R. N. Barnett and U. Landman, *J. Phys. Chem. A*, 1999, **103**, 9573–9578.
- [21] M. Daté, M. Okumura, S. Tsubota and M. Haruta, *Angew. Chem. Int. Ed.*, 2004, **43**, 2129–2132.
- [22] D. Matthey, J. G. Wang, S. Wendt, J. Matthiesen, R. Schaub, E. Lægsgaard, B. Hammer and F. Besenbacher, *Science*, 2007, **315**, 1692–1696.
- [23] A. M. Joshi, W. N. Delgass and K. T. Thomson, *J. Phys. Chem. B*, 2006, **110**, 23373–23387.
- [24] A. Lyalin and T. Taketsugu, *J. Phys. Chem. C*, 2010, **114**, 2484–2493.
- [25] J. Jia, K. Haraki, J. N. Kondo, K. Domen and K. Tamaru, *J. Phys. Chem. B*, 2000, **104**, 11153–11156.
- [26] T. V. Choudhary, C. Sivadinarayana, A. K. Datye, D. Kumar and D. W. Goodman, *Catal. Lett.*, 2003, **86**, 1.
- [27] J. E. Bailie and G. J. Hutchings, *Chem. Commun.*, 1999, 2151–2152.
- [28] S. Schimpf, M. Martin Lucas, C. Mohra, U. Rodemerck, A. Brückner, J. Radnik, H. Hofmeister and P. Claus, *Catalysis Today*, 2002, **72**, 63–78.
- [29] M. Okumura, T. Akita and M. Haruta, *Catalysis Today*, 2002, **74**, 265–269.
- [30] C. Mohr, H. Hofmeister, J. Radnik and P. Claus, *J. Am. Chem. Soc.*, 2003, **125**, 1905–1911.
- [31] R. Zanella, C. Louis, S. Giorgio and R. Touroude, *J. Catal.*, 2004, **223**, 328–339.
- [32] P. Claus, *Appl. Catal. A: Gen.*, 2005, **291**, 222–229.
- [33] Y. Zhu, H. Qian, B. A. Drake and R. Jin, *Angew. Chem. Int. Ed.*, 2010, **49**, 1295–1298.
- [34] Y. Zhu, Z. Wu, C. Gayathri, H. Qian, R. R. Gil and R. Jin, *J. Catal.*, 2010, **271**, 155–160.

- [35] E. Bus, J. T. Miller and J. A. van Bokhoven, *J. Phys. Chem. B*, 2005, **109**, 14581–14587.
- [36] C. Mohr, H. Hofmeister and P. Claus, *J. Catal.*, 2003, **213**, 86–94.
- [37] T. Fujitani, I. Nakamura, T. Akita, M. Okumura and M. Haruta, *Angew. Chem. Int. Ed.*, 2009, **48**, 9515–9518.
- [38] L. Andrews, X. Xuefeng Wang, L. Manceron and K. Balasubramanian, *J. Phys. Chem. A*, 2004, **108**, 2936–2940.
- [39] L. Andrews, *Chem. Soc. Rev.*, 2004, **33**, 123–132.
- [40] A. Zanchet, O. Roncero, S. Omar, M. Paniagua and A. Aguado, *J. Chem. Phys.*, 2010, **132**, 034301/1–10.
- [41] S. A. Varganov, R. M. Olson, M. S. Gordon, G. Mills and H. Metiu, *J. Chem. Phys.*, 2004, **120**, 5169–5175.
- [42] M. Okumura, Y. Kitagawa, M. Haruta and K. Yamaguchi, *Appl. Catal. A: Gen.*, 2005, **291**, 37–44.
- [43] L. Barrio, P. Liu, J. A. Rodríguez, J. M. Campos-Martín and J. L. G. Fierro, *J. Chem. Phys.*, 2006, **125**, 164715/1–5.
- [44] H. W. Ghebriel and A. Kshirsagar, *J. Chem. Phys.*, 2007, **126**, 244705/1–9.
- [45] A. M. Joshi, W. N. Delgass and K. T. Thomson, *Topics in Catalysis*, 2007, **44**, 27–39.
- [46] A. Corma, M. Boronat, S. González and F. Illas, *Chem. Commun.*, 2007, 3371–3373.
- [47] D. H. Wells, Jr., W. N. Delgass and K. T. Thomson, *J. Catal.*, 2004, **225**, 69–77.
- [48] K. A. Kacprzak, J. Akola and H. Häkkinen, *Phys. Chem. Chem. Phys.*, 2009, **11**, 6359–6364.
- [49] Z. Li, Z.-X. Chen, X. He and G.-J. Kang, *J. Chem. Phys.*, 2010, **132**, 184702/1–5.
- [50] X.-F. Yang, A.-Q. Wang, Y.-L. Wang, T. Zhang and J. Li, *J. Phys. Chem. C*, 2010, **114**, 3131–3139.
- [51] M. Boronat, F. Illas and A. Corma, *J. Phys. Chem. A*, 2009, **113**, 3750–3757.
- [52] E. Florez, T. Gomez, P. Liu, J. A. Rodríguez and F. Illas, *Chem. Cat. Chem.*, 2010, **2**, 1219–1222.
- [53] J. P. Perdew, K. Burke and M. Ernzerhof, *Phys. Rev. Lett.*, 1996, **77**, 3865–3868.
- [54] E. Artacho, D. Sánchez-Portal, P. Ordejón, A. García and J. M. Soler, *Phys. Stat. Sol. (b)*, 1999, **215**, 809–817.



- [55] J. Junquera, O. Paz, D. Sánchez-Portal and E. Artacho, *Phys. Rev. B*, 2001, **64**, 235111/1–9.
- [56] N. Troullier and J. L. Martins, *Phys. Rev. B*, 1991, **43**, 1993–2006.
- [57] L. Kleinman and D. M. Bylander, *Phys. Rev. Lett.*, 1982, **48**, 1425–1428.
- [58] D. Sánchez-Portal, P. Ordejón, E. Artacho and J. M. Soler, *Int. J. Quantum Chem.*, 1997, **65**, 453–461.
- [59] J. M. Soler, E. Artacho, J. D. Gale, A. García, J. Junquera, P. Ordejón and D. Sánchez-Portal, *J. Phys.: Condens. Matter*, 2002, **14**, 2745–2779.
- [60] D. Sánchez-Portal, P. Ordejón and E. Canadell, *Structure and Bonding*, 2004, **113**, 103–170.
- [61] K. P. Huber and G. Herzberg, *Molecular Spectra and Molecular Structure Constants of Diatomic Molecules*, Van Nostrand Reinhold, New York, 1979.
- [62] B. Morosin, *J. Appl. Cryst.*, 1968, **1**, 123–124.
- [63] P. Haas, F. Tran and P. Blaha, *Phys. Rev. B*, 2009, **79**, 085104/1–10.
- [64] X. Ding, Z. Li, J. Yang, J. G. Hou and Q. Zhu, *J. Chem. Phys.*, 2004, **120**, 9594–9600.
- [65] E. Fernández, J. M. Soler, I. L. Garzón and L. C. Balbás, *Phys. Rev. B*, 2004, **70**, 165403/1–14.
- [66] A. W. Walker, *J. Chem. Phys.*, 2005, **122**, 094310/1–12.
- [67] L. Xiao, B. Tollberg, X. Hu and L. Wang, *J. Chem. Phys.*, 2006, **124**, 114309/1–10.
- [68] H. Häkkinen, *Chem. Soc. Rev.*, 2008, **37**, 1847–1859.
- [69] J. A. Nelder and R. Mead, *The Computer Journal*, 1965, **7**, 308–313.
- [70] J. K. Burdett, T. Hughbanks, G. J. Miller, J. W. Richardson, Jr. and J. V. Smith, *J. Am. Chem. Soc.*, 1987, **109**, 3639–3646.
- [71] J. Muscat, V. Swamy and N. M. Harrison, *Phys. Rev. B*, 2002, **65**, 224112/1–15.
- [72] H. J. Monkhorst and J. D. Pack, *Phys. Rev. B*, 1976, **13**, 5188.
- [73] H. Perron, C. Domain, J. Roques, R. Drot, E. Simoni and H. Catalette, *Theor. Chem. Acc.*, 2007, **117**, 565–574.
- [74] T. Bredow, L. Giordano, F. Cinquini and G. Pacchioni, *Phys. Rev. B*, 2004, **70**, 035419/1–6.
- [75] M. Ramamoorthy, D. Vanderbilt and K.-S. R.D., *Phys. Rev. B*, 1994, **49**, 16721–16727.
- [76] L. M. Liu, B. McAllister, H. Q. Ye and P. Hu, *J. Am. Chem. Soc.*, 2006, **128**, 4017–4022.

- [77] Y. Wang and X. G. Gong, *J. Chem. Phys.*, 2006, **125**, 124703/1–12.
- [78] G.-J. Kang, Z.-X. Chen, Z. Li and X. He, *J. Chem. Phys.*, 2009, **130**, 034701/1–6.
- [79] A. Zanchet, A. Dorta-Urra, O. Roncero, F. Flores, C. Tablero, M. Paniagua and A. Aguado, *Phys. Chem. Chem. Phys.*, 2009, **11**, 10122–10131.
- [80] P. Pyykkö, *Chem. Soc. Rev.*, 2008, **37**, 1967–1997.
- [81] H. Häkkinen, B. Yoon, U. Landman, X. Li, H. Zhai and L. Wang, *Phys. Chem. A*, 2003, **107**, 6168–6175.
- [82] B. Assadollahzadeh and P. Schwerdtfeger, *J. Chem. Phys.*, 2009, **131**, 064306/1–11.
- [83] H. Häkkinen, M. Moseler and U. Landman, *Phys. Rev. Lett.*, 2002, **89**, 033401/1–4.
- [84] R. M. Olson, S. Varganov, M. S. Gordon, H. Metiu, S. Chretien, P. Piecuch, K. Kowalski, S. A. Kucharski and M. Musial, *J. Am. Chem. Soc.*, 2005, **127**, 1049–1052.
- [85] Y.-K. Han, *J. Chem. Phys.*, 2006, **124**, 024316/1–3.
- [86] Y. C. Choi, W. Y. Kim, H. M. Lee and K. S. Kim, *J. Chem. Theory Comput.*, 2009, **5**, 1216–1223.
- [87] A. Martínez, *J. Phys. Chem. C*, 2010, **114**, 21240–21246.
- [88] A. Lyalin and T. Taketsugu, *AIP Conference Proceedings*, 2009, **1197**, 65–75.
- [89] V. V. Semenikhina, A. Lyalin, A. V. Solov'yov and W. Greiner, *JETP*, 2008, **106**, 678–689.
- [90] D. Ricci, A. Bongiorno, G. Pacchioni and U. Landman, *Phys. Rev. Lett.*, 2006, **97**, 036106/1–4.
- [91] R. Bader, *Atoms in Molecules: A Quantum Theory*, Oxford University Press, New York, 1990.
- [92] G. Henkelman, A. Arnaldsson and H. Jónsson, *Comput. Mater. Sci.*, 2006, **36**, 354–360.
- [93] C. Bréchnignac, P. Cahuzac, M. de Frutos, N. Kébaïli, A. Sarfati and V. Akulin, *Phys. Rev. Lett.*, 1996, **77**, 251254.
- [94] C. Bréchnignac, P. Cahuzac, N. Kébaïli and J. Leygnier, *Phys. Rev. Lett.*, 1998, **81**, 4612–4615.
- [95] O. I. Obolensky, A. G. Lyalin, A. V. Solov'yov and W. Greiner, *Phys. Rev. B*, 2005, **72**, 085433/1–11.
- [96] B. Yoon, H. Häkkinen, U. Landman, A. S. Wörz, J.-M. Antonietti, S. Abbet, K. Judai and U. Heiz, *Science*, 2005, **307**, 403–407.
- [97] S. Chretien and H. Metiu, *J. Chem. Phys.*, 2007, **126**, 104701/1–7.